Inorg. Chem. **2002**, *41*, 6560–6572

NMR Shielding Calculations across the Periodic Table: Diamagnetic Uranium Compounds. 2. Ligand and Metal NMR

Georg Schreckenbach*

Theoretical Division (MS B268) and Seaborg Institute for Transactinium Science, Los Alamos National Laboratory, Los Alamos, New Mexico 87545

Received May 29, 2002

In this and a previous article (*J. Phys. Chem. A* **2000**, *104*, 8244), the range of application for relativistic density functional theory (DFT) is extended to the calculation of nuclear magnetic resonance (NMR) shieldings and chemical shifts in diamagnetic actinide compounds. Two relativistic DFT methods are used, ZORA ("zeroth-order regular approximation") and the quasirelativistic (QR) method. In the given second paper, NMR shieldings and chemical shifts are calculated and discussed for a wide range of compounds. The molecules studied comprise uranyl complexes, $[UO_2L_n]^{\pm q}$; UF_6; inorganic UF_6 derivatives, $UF_{6-n}Cl_n$, $n = 0–6$; and organometallic UF_6 derivatives, $UF_{6-n}(OCH_3)_n$, $n = 0–5$. Uranyl complexes include $[UO_2F_4]^{2-}$, $[UO_2Cl_4]^{2-}$, $[UO_2(OH)_4]^{2-}$, $[UO_2(CO_3)_3]^{4-}$, and $[UO_2(H_2O)_5]^{2+}$. For the ligand NMR, moderate (e.g., ^{19}F NMR chemical shifts in $UF_{6-n}Cl_n$) to excellent agreement [e.g., ^{19}F chemical shift tensor in UF_6 or ^1H NMR in $UF_{6-n}(OCH_3)_n$] has been found between theory and experiment. The methods have been used to calculate the experimentally unknown ^{235}U NMR chemical shifts. A large chemical shift range of at least 21 000 ppm has been predicted for the ^{235}U nucleus. ZORA spin–orbit appears to be the most accurate method for predicting actinide metal chemical shifts. Trends in the ^{235}U NMR chemical shifts of $UF_{6-n}L_n$ molecules are analyzed and explained in terms of the calculated electronic structure. It is argued that the energy separation and interaction between occupied and virtual orbitals with f-character are the determining factors.

1. Introduction

The calculation of nuclear magnetic resonance (NMR) shieldings and chemical shifts from first-principle quantum mechanics has recently seen a rapid development.[1−6] During the past decade or so, tremendous progress has been achieved in at least two directions. First, various developments aim at increasing the accuracy of the calculations, in particular by accounting for the effects of electron correlation.[1,4] Second, the range of applications has been gradually extended from light organic compounds toward the lower part of the periodic table and—very recently—toward transition metal compounds.[5,7]

Density functional theory[8−11] (DFT) has been central in these developments. This is particularly true for applications to large (transition) metal complexes and other extended systems.[5−7] Regarding metal complexes, NMR calculations have been done both on light ligand nuclei (e.g., refs 12−18; for a review, see ref 7) and on the heavy nucleus proper. Examples in the latter category include studies on

* New address: Department of Chemistry and Biochemistry, Concordia University, 1455 de Maisonneuve Blvd. West, Montreal, Quebec, Canada, H3G 1M8. E-mail: schrecke@alcor.concordia.ca.

(1) Helgaker, T.; Jaszunski, M.; Ruud, K. *Chem. Rev.* **1999**, *99*, 293−352.
(2) Chesnut, D. B. In *Annual Reports on NMR Spectroscopy;* Webb, G. A., Ed.; Academic Press: New York, 1994; Vol. 29, pp 71−122.
(3) Chesnut, D. B. In *Reviews in Computational Chemistry*; Libkowitz, K. B., Boyd, D. B., Eds.; Verlag Chemie: Weinheim (Germany), New York, 1996; Vol. 8, pp 245−297.
(4) Gauss, J. *Ber. Bunsen-Ges. Phys. Chem.* **1995**, *99*, 1001.
(5) Schreckenbach, G.; Ziegler, T. *Theor. Chem. Acc.* **1998**, *99*, 71−82.
(6) Bühl, M.; Kaupp, M.; Malkin, V. G.; Malkina, O. L. *J. Comput. Chem.* **1999**, *20*, 91−105.
(7) Kaupp, M.; Malkina, O. L.; Malkin, V. G. In *Encyclopedia of Computational Chemistry*; Schleyer, P. v. R., Allinger, N. L., Clark, T., Gasteiger, J., Kollman, P. A., Schaefer, H. F., III, Scheiner, P. R., Eds.; John Wiley & Sons: New York, 1998; Vol. 3, pp 1857−1866.
(8) Hohenberg, P.; Kohn, W. *Phys. Rev.* **1964**, *136*, B864.
(9) Kohn, W.; Sham, L. J. *Phys. Rev.* **1965**, *140*, A1133.
(10) Parr, R. G.; Yang, W. *Density-Functional Theory of Atoms and Molecules*; Oxford University Press: New York, Oxford, 1989.
(11) Ziegler, T. *Chem. Rev.* **1991**, *91*, 651−667.
(12) Kaupp, M.; Malkin, V. G.; Malkina, O. L.; Salahub, D. R. *J. Am. Chem. Soc.* **1995**, *117*, 1851−1852.
(13) Kaupp, M.; Malkina, O. L.; Malkin, V. G. *Chem. Phys. Lett.* **1997**, *265*, 55−59.
(14) Schreckenbach, G.; Ziegler, T. *Int. J. Quantum Chem.* **1997**, *61*, 899.
(15) Ruiz-Morales, Y.; Schreckenbach, G.; Ziegler, T. *J. Phys. Chem.* **1996**, *100*, 3359−3367.
(16) Ruiz-Morales, Y.; Schreckenbach, G.; Ziegler, T. *Organometallics* **1996**, *15*, 3920.

10.1021/ic020370j CCC: $22.00
Published on Web 11/14/2002

the metal NMR shieldings and chemical shifts of compounds containing the chromium[14] (^{53}Cr), iron[19−21] (^{57}Fe), cobalt[22,23] (^{59}Co), selenium[24−26] (^{77}Se), zirconium[27,28] (^{91}Zr), molybdenum[14,17] (^{95}Mo/^{97}Mo), rhodium[20,29] (^{103}Rh), tellurium[30] (^{125}Te), tungsten[14,31] (^{183}W), platinum[32] (^{195}Pt), mercury[33] (^{199}Hg), and lead[31] (^{207}Pb) nuclei, among others.[34−36] As is evident from this list, applications to transition metals and heavy p-block elements are now becoming possible for the first time. Consequently, this area is being actively explored.

In the theoretical study of metal complexes, be it main group, transition metal, lanthanide, or actinide complexes, electron correlation effects have to be accounted for. This explains why almost all of the cited papers[12−23,26−33] employed DFT,[37] as DFT allows for an efficient treatment of electron correlation.[11] For compounds containing heavier nuclei, it becomes, in addition, necessary to include relativistic effects as well. It is relatively straightforward to include such effects into DFT—another advantage of the method.[38]

With this article and a preceding paper[39] (hereafter "Part 1"), the theoretical work on the NMR of metal complexes will be extended. The heaviest part of the periodic table, i.e., the f-block elements will be covered. Diamagnetic (i.e., formally f^0) uranium compounds have been chosen as a representative example. To the best of my knowledge, NMR shieldings and chemical shifts in compounds of the lanthanide or actinide elements have never been studied before by first principle theoretical methods.[40,41]

Recently, there has been a strong interest in studying actinide chemistry from first-principle quantum mechanics.[38,42,43] This attention is based on both fundamental and practical considerations. Fundamental interest arises because f-orbitals can participate in bonding, leading to unique new bonding schemes, but also because actinide chemistry remains one of the most challenging and difficult areas for electronic structure theory.[38,42] Practical interest is primarily due to the radioactivity of the actinide elements, making experimental investigations exceedingly difficult. Hence, in this area of chemistry, theory has a particularly strong potential of providing useful data that might supplement and extend experimental findings.

In this paper, two different relativistic DFT methods were employed, the "quasirelativistic" (QR) method,[44,45] which employs a Pauli Hamiltonian,[46] and the more modern "zeroth-order relativistic approximation" (ZORA) for relativistic effects.[47−50]

In the first paper of the series,[39] attempts were made to evaluate different relativistic approximations, including the QR and ZORA approaches. Both QR and ZORA were shown to be reliable, with ZORA being somewhat more accurate. Further, a number of issues were discussed that arise in the calculation of NMR chemical shifts in actinide compounds. In addition, already some limited results were presented. Thus, the ^{19}F NMR in $UF_{6-n}Cl_n$ ($n = 0-5$) compounds and the ^{19}F NMR chemical shift tensor in UF_6 have been discussed. Agreement with experiment was found to be satisfactory for the latter case, whereas the calculations missed certain trends in the fluorine NMR along the fluoride chloride series.

In the given second paper of the series, the methods that were established in the first paper will be applied to a wide

(17) Ruiz-Morales, Y.; Ziegler, T. *J. Phys. Chem. A* **1998**, *102*, 3970−3976.
(18) Wolff, S. K.; Ziegler, T. *J. Chem. Phys.* **1998**, *109*, 895−905.
(19) Bühl, M.; Malkin, V. G.; Malkina, O. L. *Helv. Chim. Acta* **1996**, *79*, 742.
(20) Bühl, M. *Chem. Phys. Lett.* **1997**, *267*, 251−257.
(21) Schreckenbach, G. *J. Chem. Phys.* **1999**, *110*, 11936−11949.
(22) Chan, J. C. C.; Au−Yeung, S. C. F. *J. Phys. Chem. A* **1997**, *101*, 3637−3640.
(23) Godbout, N.; Oldfield, E. *J. Am. Chem. Soc.* **1997**, *119*, 8065−8069.
(24) Bühl, M.; Thiel, W.; Fleischer, U.; Kutzelnigg, W. *J. Phys. Chem.* **1995**, *99*, 4000−4007.
(25) Bühl, M.; Gauss, J.; Stanton, J. F. *Chem. Phys. Lett.* **1995**, *241*, 248−252.
(26) Schreckenbach, G.; Ruiz-Morales, Y.; Ziegler, T. *J. Chem. Phys.* **1996**, *104*, 8605.
(27) Bühl, M.; Brintzinger, H.-H.; Hopp, G. *Organometallics* **1996**, *15*, 778.
(28) Bühl, M. *J. Phys. Chem. A* **1997**, *101*, 2514−2517.
(29) Bühl, M. *Organometallics* **1997**, *16*, 261−267.
(30) Ruiz-Morales, Y.; Schreckenbach, G.; Ziegler, T. *J. Phys. Chem. A* **1997**, *101*, 4121−4127.
(31) Rodriguez-Fortea, A.; Alemany, P.; Ziegler, T. *J. Phys. Chem. A* **1999**, *103*, 8288−8294.
(32) Gilbert, T. M.; Ziegler, T. *J. Phys. Chem. A* **1999**, *103*, 7535−7543.
(33) Wolff, S. K.; Ziegler, T.; van Lenthe, E.; Baerends, E. J. *J. Chem. Phys.* **1999**, *110*, 7689−7698.
(34) Nakatsuji, H. In *Nuclear Magnetic Shieldings and Molecular Structure;* NATO ASI C386; Tossell, J. A., Ed.; Kluwer Academic Publishers: Dordrecht, The Netherlands, 1993; p 263.
(35) Nakatsuji, H.; Nakajima, T.; Hada, M.; Takashima, H.; Tanaka, S. *Chem. Phys. Lett.* **1995**, *247*, 418.
(36) Nakatsuji, H.; Hu, Z. M.; Nakajima, T. *Chem. Phys. Lett.* **1997**, *275*, 429−436.
(37) In this connection, I should also mention the early work of Nakatsuji and co-workers, who studied the NMR chemical shift of various metal nuclei; see ref 34 and references therein. Some newer papers include, for instance, refs 35 and 36. This work was typically based on the coupled Hartree−Fock (CHF) approach. Thus, the so-called "gauge problem" of magnetic properties[2] has not been addressed at all. Typically, the resulting strong gauge-dependence of the calculated NMR shieldings has been reduced by choosing highly symmetric molecules only. Furthermore, the CHF approach means that the important correlation effects have not been addressed in these studies.
(38) Schreckenbach, G.; Hay, P. J.; Martin, R. L. *J. Comput. Chem.* **1999**, *20*, 70−90.
(39) Schreckenbach, G.; Wolff, S. K.; Ziegler, T. *J. Phys. Chem. A* **2000**, *104*, 8244−8255.
(40) Preliminary results of this work have already been reported in ref 41. Please note that some of the calculated numbers in this reference are slightly wrong (by a few percent at most), due to some small program errors that have been fixed since. This concerns the Pauli spin−orbit numbers in Tables 4 and 5 of this reference. In addition, the number given in Table 5 of this reference for the absolute ^{235}U shielding of $[UO_2(OH)_4]^{2-}$ (Pauli spin−orbit) is wrong due to a typographical error. The corrected numbers are given in Table 5 of Part 1 and in Table 5 of the given paper, respectively.
(41) Schreckenbach, G.; Wolff, S. K.; Ziegler, T. In *Modeling NMR Chemical Shifts: Gaining Insight into Structure and Environment;* ACS Symposium Series 732; Facelli, J. C., de Dios, A., Eds.; American Chemical Society: Washington, DC, 1999; pp 101−114.
(42) Pepper, M.; Bursten, B. E. *Chem. Rev.* **1991**, *91*, 719−741.
(43) Dolg, M. In *Encyclopedia of Computational Chemistry*; Schleyer, P. R. v., Ed.; Wiley-Interscience: New York, 1998.
(44) Boerrigter, P. M.; Baerends, E. J.; Snijders, J. G. *Chem. Phys.* **1988**, *122*, 357−374.
(45) Ziegler, T.; Tschinke, V.; Baerends, E. J.; Snijders, J. G.; Ravenek, W. *J. Phys. Chem.* **1989**, *93*, 3050.
(46) Pauli, W. *Z. Phys.* **1927**, *43*, 601.
(47) Chang, C.; Pellisier, M.; Durand, P. *Phys. Scr.* **1986**, *34*, 394−404.
(48) van Lenthe, E.; Baerends, E. J.; Snijders, J. G. *J. Chem. Phys.* **1993**, *99*, 4597−4610.
(49) van Lenthe, E.; Baerends, E. J.; Snijders, J. G. *J. Chem. Phys.* **1994**, *101*, 9783−9792.
(50) van Lenthe, E.; van Leeuwen, R.; Baerends, E. J. *Int. J. Quantum Chem.* **1996**, *57*, 281−293.

range of (diamagnetic) uranium compounds. Specifically, I will extend my studies and consider again the inorganic fluoride chlorides $UF_{6-n}Cl_n$ ($n = 0-6$); organometallic methoxy derivatives of UF_6, $UF_{6-n}(OCH_3)_n$ ($n = 0-5$); and some examples of uranyl complexes $[UO_2L_n]^{\pm q}$, where various ligands L coordinate to the equatorial plane of the stable UO_2^{2+} unit. I will discuss calculated ligand NMR in comparison to experiment where possible. Further, I will present calculated ^{235}U NMR shieldings and chemical shifts. Only once has an NMR signal of an actinide nucleus been observed, namely for UF_6.[51] Hence, ^{235}U relative chemical shifts (or any other actinide shifts) have not yet been measured. Principally, this is due to an unfavorable signal-to-noise ratio—^{235}U is a quadrupolar nucleus—combined with the large chemical shift range and the radioactivity of the actinides. It is hoped that the present calculations might help to guide future experiments, by narrowing down the magnetic field ranges that have to be scanned for a signal. Finally, the calculations shall be used to rationalize certain trends in the calculated NMR shieldings (chemical shifts). This will be achieved by using an analysis of the chemical shift in terms of the calculated electronic structure. The ability to perform such an analysis is one particular strength of theory.

2. Relativity

Before turning to the actual calculations, I would like to qualitatively summarize how relativistic effects manifest themselves in calculated NMR shieldings and chemical shifts. The mechanisms for that are by now well understood.

Sometimes, relativistic effects on some properties like the NMR shielding have been divided into "direct" and "indirect" effects, with the latter arising from the well-known relativistic bond contraction[52] or, more generally, from differences between nonrelativistic and relativistic molecular structures. Here, I will consider fixed, relativistic geometries only and hence will not discuss the "indirect" relativistic effects any further.

The remaining "direct" relativistic effects can be divided into scalar and spin−orbit/Fermi contact effects. Furthermore, there are core and valence contributions in either case.

To start with the scalar relativistic effects, core effects on the absolute shielding result from a large increase of the diamagnetic shielding contribution due to the contraction of the inner core shells, 1s in particular.[5] The effect is mostly independent of the chemical environment of the heavy nucleus, since such core-type s- and p-orbitals are essentially unaltered upon bond formation. Hence, it cancels out in relative chemical shifts.[14] Besides, there are also valence effects arising from scalar relativity. Typically, the leading contribution to the chemical shift is due to a coupling between occupied and virtual molecular orbitals (eqs 3 and 5 below.) This coupling describes the induced paramagnetic currents in the system.[5,14,21,53] The strength of this interaction is inversely proportional to the MO energy differences, and it is easy to see that a relativistic stabilization or destabilization of certain MOs will influence these energy differences. (Similarly, contraction or expansion of certain orbitals may alter the magnitude of the magnetic matrix elements between them; see eq 5 below.) Furthermore, it follows that this relativistic effect will be relevant for both the heavy element proper and the neighboring light nuclei.[5,14]

Spin−orbit effects follow a different mechanism.[54] Thus, the relativistic spin−orbit operators, in the presence of a magnetic field, produce spin polarization at the heavy nucleus, even for formally closed-shell systems.[55] This can also be shown rigorously.[18] The spin polarization is transferred through the bond to an NMR nucleus, where it is picked up by means of a Fermi contact mechanism; see eq 6 below. One important consequence of this picture is that spin−orbit chemical shifts are only relevant if there are strong s-bond contributions at the NMR nucleus. Core contributions at the heavy nucleus proper arise because the spin−orbit-induced spin polarization is also picked up by the core-type s-orbitals at the heavy nucleus itself. Again, such core contributions cancel out in relative chemical shifts.

3. Computational Details

NMR shieldings and chemical shifts are calculated using relativistic DFT and the "gauge including atomic orbitals" (GIAO) approach.[56−58] The technical details of the methods have been discussed in the first paper of the series[39] and in the original references,[14,18,33,53,59,60] and they shall be outlined only very briefly at this point.

The Amsterdam Density Functional code ADF[61−64] has been used for all NMR calculations that are reported in this paper. As mentioned in the Introduction, relativistic effects are accounted for by means of the QR[44,45] (Pauli) or ZORA[47−50] methods, cf. ref 39. Spin−orbit effects can be included or excluded in either method. The neglect of spin−orbit effects leads to a scalar relativistic approximation.

Standard ADF basis sets are employed, as has been described in more detail previously.[39] These are Slater type basis sets that are of triple-ζ plus polarization quality in the valence region and of single-ζ (Pauli) or double-ζ (ZORA) quality in the core region.

(51) Le Bail, H.; Chachaty, C.; Rigny, P.; Bougon, R. *J. Phys. Lett.* **1983**, *44*, 1017−1019.
(52) Pyykkö, P. *Chem. Rev.* **1988**, *88*, 563−594.
(53) Schreckenbach, G.; Ziegler, T. *J. Phys. Chem.* **1995**, *99*, 606−611.
(54) Pyykkö, P.; Görling, A.; Rösch, N. *Mol. Phys.* **1987**, *61*, 195.
(55) Kaupp, M.; Malkina, O. L.; Malkin, V. G.; Pyykkö, P. *Chem. Eur. J.* **1998**, *4*, 118.
(56) London, F. *J. Phys. Radium* **1937**, *8*, 397.
(57) Ditchfield, R. *Mol. Phys.* **1974**, *27*, 789.
(58) Wolinski, K.; Hinton, J. F.; Pulay, P. *J. Am. Chem. Soc.* **1990**, *112*, 8251.
(59) Schreckenbach, G.; Ziegler, T. *Int. J. Quantum Chem.* **1996**, *60*, 753.
(60) Schreckenbach, G.; Dickson, R. M.; Ruiz-Morales, Y.; Ziegler, T. In *Chemical Applications of Density Functional Theory;* ACS Symposium Series 629; Laird, B. B., Ross, R. B., Ziegler, T., Eds.; American Chemical Society: Washington, DC, 1996; pp 328−341.
(61) Baerends, E. J.; Ellis, D. E.; Ros, P. *Chem. Phys.* **1973**, *2*, 41.
(62) te Velde, G.; Baerends, E. J. *J. Comput. Phys.* **1992**, *99*, 84−98.
(63) Fonseca Guerra, C.; Snijders, J. G.; te Velde, G.; Baerends, E. J. *Theor. Chem. Acc.* **1998**, *99*, 391−403.
(64) Baerends, E. J.; Bérces, A.; Bo, C.; Boerrigter, P. M.; Cavallo, L.; Deng, L.; Dickson, R. M.; Ellis, D. E.; Fan, L.; Fischer, T. H.; Fonseca Guerra, C.; van Gisbergen, S. J. A.; Groeneveld, J. A.; Gritsenko, O. V.; Harris, F. E.; van den Hoek, P.; Jacobsen, H.; van Kessel, G.; Koostra, F.; van Lenthe, E.; Osinga, V. P.; Philipsen, P. H. T.; Post, D.; Pye, C. C.; Ravenek, W.; Ros, P.; Schipper, P. R. T.; Schreckenbach, G.; Snijders, J. G.; Sola, M.; Swerhone, D.; te Velde, G.; Vernooijs, P.; Versluis, L.; Visser, O.; van Wezenbeek, E.; Wiesenekker, G.; Wolff, S. K.; Woo, T. K.; Ziegler, T. ADF99 *Theoretical Chemistry;* Vrije Universiteit: Amsterdam, The Netherlands, 1999.

Furthermore, the frozen core approximation[61] is applied in Pauli (QR) calculations.[44,45] Here, all shells up to and including the 1s (C, O, F), 2p (Cl), and 5d shells (U), respectively, are considered as core and kept frozen in molecular calculations. In ZORA calculations, all electrons are treated variationally. Again, see the first paper of the series[39] for a detailed description and discussion of these settings.

For the XC functional of DFT, the generalized gradient approximation (GGA) due to Perdew and Wang[65] has been used (PW91). As has been discussed in previously,[39] relativistic corrections to the XC functional[66,67] have been neglected. Similarly, no current dependent terms[68−70] have been included into the XC functional, leading to the so-called "uncoupled" DFT.[5]

The NMR shielding tensor is well-known to be "sensitive to everything" (cf. Part 1), including the reference geometry at which the calculation is performed.[1] I prefer to use high-quality experimental geometries, in cases where such data is available. However, no experimental structural data is available for most of the compounds that were chosen for this study. Hence, I decided to use optimized geometries throughout. The only exception is tetramethylsilane (TMS), where I used the accurate experimental geometry (as obtained from electron diffraction measurements, r_g geometry) due to Beagley et al.;[71] see Part 1.[72] For consistency, I used the same approach as in previous structural studies.[38,41,73,74] In particular, all structures were optimized with the GAUSSIAN94 program system.[75] I employed an effective core potential (ECP) on uranium,[76] together with the respective general ECP basis set in its totally uncontracted form. The 6-31+G* all-electron Gaussian basis set was applied on all (light) ligand atoms. With this choice of basis set, geometry optimizations were performed using DFT and the B3LYP hybrid XC functional.[77,78] Previous studies have shown that this combination gave good agreement between theory and experiment for a number of test cases.[38,73,74] In these studies, the experimental bond lengths were typically still overestimated to some degree. The optimized geometries and vibrational frequencies of $[UO_2(OH)_4]^{2-}$, $[UO_2F_4]^{2-}$, $[UO_2Cl_4]^{2-}$, UF_6, and $UF_{6-n}L_n$ series ($n = 0-6$, L = Cl and OCH_3) have been published already elsewhere.[38,73,74] I include the optimized geometries of the remaining molecules ($[UO_2(CO_3)_3]^{4-}$ $[UO_2(H_2O)_5]^{2+}$) as Supporting Information.

4. Analysis of the Shielding

As mentioned in the Introduction, a particular strength of theoretical approaches in general, and of the DFT-GIAO method in particular, is that they allow an analysis of the calculated shieldings and chemical shifts in terms of the electronic structure. In the following, I shall briefly outline my approach to this analysis. I will make no attempt to present the theory completely. Rather, I would like to show only those equations that are relevant for the analysis of the calculated shieldings. For a more detailed account of the theory, the reader may refer to Part 1[39] and, in particular, to the original references.[14,18,33,53,59,60]

The theoretical property, the shielding tensor σ, is related to the experimentally observed chemical shift tensor, δ, by the following relation

$$\delta = \sigma_{\mathrm{ref}} - \sigma \tag{1}$$

where σ and δ are isotropic averages (one-third of the traces) of the tensors and σ_{ref} is the absolute shielding of the reference compound (e.g., tetramethylsilane, TMS, for ^{1}H and ^{13}C NMR). I will cite results in either form, as chemical shifts or as absolute shieldings. Note the opposite sign between changes to σ and δ.

The NMR shielding tensor can be written as a sum of three contributions[14,18,33,53,59,60]

$$\vec{\vec{\sigma}} = \vec{\vec{\sigma}}^{\mathrm{d}} + \vec{\vec{\sigma}}^{\mathrm{so}} + \vec{\vec{\sigma}}^{\mathrm{p}} \tag{2}$$

The terms in eq 2 are, respectively, the diamagnetic, (relativistic) spin−orbit, and paramagnetic contributions. The diamagnetic shielding depends on the zero-order electronic density only. The paramagnetic shielding, however, is determined by the magnetically perturbed MOs. Within the GIAO formalism, these magnetic orbitals can be described by the density matrix to first order in the magnetic field that, in turn, is expanded into the occupied and virtual MOs. The leading contribution couples occupied and virtual MOs, and one can write, at least approximately (*ts* tensor component)

$$\sigma_{\mathrm{ts}}^{\mathrm{p}} \propto \sigma_{\mathrm{ts}}^{\mathrm{p,oc-vir}} = 2\sum_{i}^{\mathrm{occ}} n_i \sum_{a}^{\mathrm{vir}} u_{ai}^{1,s} \langle \Psi_i | h_{\mathrm{t}}^{01} | \Psi_a \rangle \tag{3}$$

In this equation, Ψ_a and Ψ_i describe virtual and occupied MOs (with occupation number n_i), respectively, and h_t^{01} is given by

$$h_{\mathrm{t}}^{01} = \frac{\mathrm{i}}{c}\left[\frac{\vec{r}_{\mathrm{N}}}{r_{\mathrm{N}}^{3}} \times \vec{p}\right]_t \tag{4}$$

Further, c is the speed of light, $\vec{r}_{\mathrm{N}}$ is the electronic position operator relative to the NMR nucleus N, and $\vec{p}$ is the electronic momentum operator. The leading contribution to

(65) Perdew, J.; Wang, Y. *Phys. Rev. B: Condens. Matter* **1992**, *45*, 13244.
(66) Engel, E.; Dreizler, R. M. *Top. Curr. Chem.* **1996**, *181*, 1−80.
(67) Mayer, M.; Häberlen, O. D.; Rösch, N. *Phys. Rev. A* **1996**, *54*, 4775−4782.
(68) Rajagopal, A. K.; Callaway, J. *Phys. Rev. B* **1973**, *7*, 1912−1919.
(69) Rajagopal, A. K. *J. Phys. C* **1978**, *11*, L943.
(70) Lee, A. M.; Handy, N. C.; Colwell, S. M. *J. Chem. Phys.* **1995**, *103*, 10095.
(71) Beagley, B.; Monaghan, J. J.; Hewitt, T. G. *J. Mol. Struct.* **1971**, *8*, 401−411.
(72) One could argue that, for consistency, optimized geometries should be used for *all* molecules, including the reference compound TMS. This argument would be based on the well-known geometry dependence of the NMR shieldings. It would be correct if the geometry dependence was similar for TMS on one hand, and the uranium complexes on the other. However, it is unlikely that this is the case, given the entirely different bonding situations and electronic structure. Hence, it appears that, instead, the strategy of using the best available geometry is preferable. For the actinide systems, this means optimized geometries. Yet for TMS, the best available geometry is the experimental structure.[71] The difference is, in any case, rather small.[39]
(73) Schreckenbach, G.; Hay, P. J.; Martin, R. L. *Inorg. Chem.* **1998**, *37*, 4442−4451.
(74) Schreckenbach, G. *Inorg. Chem.* **2000**, *39*, 1265−1274.
(75) Frisch, M. J.; Trucks, G. W.; Schlegel, H. B.; Gill, P. M. W.; Johnson, B. G.; Robb, M. A.; Cheeseman, J. R.; Keith, T.; Petersson, G. A.; Montgomery, J. A.; Raghavachari, K.; Al-Laham, M. A.; Zakrzewski, V. G.; Ortiz, J. V.; Foresman, J. B.; Cioslowski, J.; Stefanov, B. B.; Nanayakkara, A.; Challacombe, M.; Peng, C. Y.; Ayala, P. Y.; Chen, W.; Wong, M. W.; Andres, J. L.; Replogle, E. S.; Gomperts, R.; Martin, R. L.; Fox, D. J.; Binkley, J. S.; Defrees, D. J.; Baker, J.; Stewart, J. P.; Head-Gordon, M.; Gonzalez, C.; Pople, J. A. Gaussian94, Revision E.1; Gaussian, Inc.: Pittsburgh, PA, 1995.
(76) Hay, P. J.; Martin, R. L. *J. Chem. Phys.* **1998**, *109*, 3875−3881.
(77) Becke, A. D. *J. Chem. Phys.* **1993**, *98*, 5648−5652.
(78) Lee, C.; Yang, W.; Parr, R. G. *Phys. Rev. B* **1988**, *37*, 785.

the first-order coefficient $u_{ai}^{1,s}$ is given as

$$u_{ai}^{1,s} \propto -\frac{1}{\epsilon_i^{(0)} - \epsilon_a^{(0)}} \sum_{\lambda,\nu}^{2M} d_{\lambda a}{}^0 d_{\nu i}{}^0 \{\langle \chi_\lambda | [\vec{r}_\nu \times \vec{\nabla}]_s | \chi_\nu \rangle \propto -\frac{1}{\epsilon_i^{(0)} - \epsilon_a^{(0)}} \langle \Psi_i | \hat{M}_s | \Psi_a \rangle \quad (5)$$

Here, the $\{d_{\beta i}\}$ are the expansion coefficients of the MOs into the primitive basis functions $\{\chi_\beta\}$ (atomic orbitals AO), $\vec{r}_\nu = \vec{r} - \vec{R}_\nu$ is the electronic position operator with respect to the position of the AO χ_ν, $\epsilon_p^{(0)}$ is the MO energy (i.e., the Kohn−Sham eigenvalue of orbital Ψ_p in the unperturbed, field-free case), and atomic units and the Gaussian unit system have been used in eqs 3−5. Within the GIAO approach, the action of the "magnetic" operator $\hat{M}_s$ on an MO Ψ_q is to work with iL_ν^s on each constituting AO χ_ν, L_ν^s being the s-component of the electronic angular momentum operator about the position $\vec{R}_\nu$ of χ_ν. Tabulations of $L_\nu^s \chi_\nu$ have been published.[79,80] Note from eq 5 that the paramagnetic shielding is inversely proportional to the MO energy difference $\epsilon_i^{(0)} - \epsilon_a^{(0)}$. Further, notice the localized nature of the shielding that is manifested in the $1/r_N^2$ dependence in eq 4.

As has been discussed qualitatively above, the spin−orbit shielding contribution, $\vec{\vec{\sigma}}^{so}$ of eq 2, is dominated by the Fermi contact term[18] that depends on the spin polarization at the NMR nucleus (ts tensor component)

$$\sigma_{ts}^{so} \propto \sigma_{ts}^{FC} = \frac{4\pi g}{3c} \sum_i^{occ} \sum_a^{vir} u_{ai}^{1,s} \langle \Psi_a | \hat{S}_t \delta(\vec{r}_N = 0) | \Psi_i \rangle \quad (6)$$

where g is the electronic Zeeman g-factor, and $\hat{S}_+$ is a Cartesian component of the electronic spin operator. Note that eq 6 has been given here for the Pauli (QR) approach.[18] The ZORA formulation of the NMR shielding tensor contains similar terms.[33]

5. Results and Discussion

Building on the discussion of the previous paper in the series,[39] I have applied the relativistic DFT-NMR methods (QR and ZORA) to a range of diamagnetic uranium compounds. The goal is to cover different bonding situations and thus to create a comprehensive picture. I will start the discussion with ligand NMR shieldings and chemical shifts and will go on to the calculated ^{235}U NMR.

(A) Uranyl Complexes $[UO_2L_n]^{\pm q}$. The very stable linear actinyl unit $AnO_2^{1+/2+}$ is ubiquitous in the chemistry of the early actinides An.[81] Typically, several ligands L can be found in the equatorial plane of the actinyl complexes.

I have calculated the NMR shieldings for five such complexes of uranyl, UO_2^{2+}. The results are collected in Tables 1 and 2, where they are also compared to the available experimental data.[82,83] Note that I have converted the experimental chemical shifts to absolute shieldings, according to eq 1. Absolute shielding scales have been used for this purpose, as explained in a footnote to the tables.[84−87]

Table 1. Diamagnetic Uranyl Complexes $[UO_2L_n]^{\pm q}$: ^{17}O NMR of the Uranyl Oxygen

	absolute NMR shielding (ppm)				
		calculated (Pauli)		calculated (ZORA)	
molecule	experiment[a]	scalar	spin−orbit	scalar	spin−orbit
$[UO_2F_4]^{2-}$		−735.2	−737.6	−752.8	−768.0
$[UO_2Cl_4]^{2-}$		−718.8	−713.4	−732.7	−747.5
$[UO_2(H_2O)_5]^{2+}$	−830[b]	−726.0	−716.5	−738.1	−756.1
$[UO_2(OH)_4]^{2-}$	−826[c]	−702.4	−704.1	−723.5	−737.6
$[UO_2(CO_3)_3]^{4-}$	−807[b]	−693.5	−689.6	−710.4	−724.1

[a] Experimental numbers from refs 82 and 83. Experimental chemical shifts have been converted to absolute shieldings, based on an absolute shielding scale.[84] A theoretical value of σ(^{17}O, liquid water, room temperature) = 290.9 ppm was used.[85,86] This value is based on the accurate, rovibrationally averaged CCSD(T) calculations of Sundholm et al.[85] for CO and the experimental chemical shift between gaseous CO and liquid water.[87] [b] Reference 82. [c] Reference 83. It is likely that this experimental value refers to the pentahydroxide, $[UO_2(OH)_5]^{3-}$, or a mixture of $[UO_2(OH)_4]^{2-}$ and $[UO_2(OH)_5]^{3-}$; see the text.

Table 2. Ligand Absolute Shieldings in Uranyl Tricarbonate, $[UO_2(CO_3)_3]^{4-}$ (ppm)

	absolute shielding				
		calculated (Pauli)		calculated (ZORA)	
nucleus	experiment[a]	scalar	spin−orbit	scalar	spin−orbit
^{17}O(=U)	−807	−693.5	−689.6	−710.4	−724.1
^{17}O(−C) bridging		−14.4	−16.3	−26.5	−10.5
^{17}O(−C) terminal		66.7	62.3	62.5	55.6
^{17}O(−C) average	66	12.6	9.9	3.2	11.6
^{13}C	18.4	−1.1	−1.8	0.0	0.4

[a] Experimental numbers from ref 82. Experimental chemical shifts have been converted to absolute shieldings, based on absolute shielding scales.[84] An experimental value of σ(^{13}C, TMS) = 184.1 ppm[84] and a theoretical value of σ(^{17}O, liquid water, room temperature) = 290.9 ppm were used.[85−87] (See also footnote *a* of Table 1.)

Let us start with the ^{17}O shielding of the uranyl oxygen (Table 1). The effect of spin−orbit is seen to be relatively minor in this case. Interestingly, the ZORA spin−orbit terms and the Pauli spin−orbit/Fermi contact terms appear to have the opposite sign in some cases. A similar effect had been found in Part 1 for the ^{19}F NMR in mixed uranium fluoride chloride systems.

Experimental data is available for the tricarbonate,[82] pentaaquo,[82] and hydroxide complexes.[83] Note that all the

(79) Ballhausen, C. J. *Introduction to Ligand Field Theory*; McGraw-Hill: New York, 1962.
(80) McGlynn, S. P.; Vanquickenborne, L. G.; Kinoshita, M.; Carroll, D. G. *Introduction to Applied Quantum Chemistry*; Holt, Rinehart and Winston: New York, 1972.
(81) Denning, R. G. *Struct. Bonding (Berlin)* **1992**, *79*, 215.
(82) Allen, P. G.; Bucher, J. J.; Clark, D. L.; Edelstein, N. M.; Ekberg, S. A.; Gohdes, J. W.; Hudson, E. A.; Kaltsoyannis, N.; Lukens, W. W.; Neu, M. P.; Palmer, P. D.; Reich, T.; Shuh, D. K.; Tait, C. D.; Zwick, B. D. *Inorg. Chem.* **1995**, *34*, 4797−4807.
(83) Clark, D. L.; Conradson, S. D.; Donohoe, R. J.; Keogh, D. W.; Morris, D. E.; Palmer, P. D.; Rogers, R. D.; Tait, C. D. *Inorg. Chem.* **1999**, *38*, 1456−1466.
(84) Jameson, C. J. In *Encyclopedia of Nuclear Magnetic Resonance*; Grant, D. M., Harris, R. K., Eds.; John Wiley & Sons: New York, 1996; pp 1273−1281.
(85) Sundholm, D.; Gauss, J.; Schäfer, A. *J. Chem. Phys.* **1996**, *105*, 11051−11059.
(86) Kaupp, M.; Malkina, O. L.; Malkin, V. G. *J. Chem. Phys.* **1997**, *106*, 9201−9212.
(87) Wasylishen, R. E.; Mooibroek, S.; Macdonald, J. B. *J. Chem. Phys.* **1984**, *81*, 1057−1059.

theoretical methods correctly predict the experimental trend in the ^{17}O shielding of these compounds, $\sigma([UO_2(H_2O)_5]^{2+}) < \sigma([UO_2(OH)_4]^{2-}) < \sigma([UO_2(CO_3)_3]^{4-})$. On the other hand, all calculations underestimate the experimental shieldings in absolute terms. ZORA spin−orbit calculations give the best agreement. The average deviation between theory and experiment is 82 ppm (118 ppm for Pauli spin−orbit).

The source of this systematic error is not entirely clear. As has also been discussed in Part 1,[39] the following error sources may contribute in principle: solvation effects, dynamic processes (such as chemical exchange), the choice of approximate XC functional, and errors in the optimized geometries.

Solvation effects in particular have been neglected here but are expected to be the reason for at least part of the deviation between theory and experiment. Solvation effects have been identified in the first part of the series as one of the issues that influence the calculation of NMR shieldings and chemical shifts. For instance, the uranyl oxygens will form hydrogen bonds to neighboring solvent molecules. In addition, experimental studies of the uranyl(VI) ion under highly alkaline aqueous conditions indicate that two hydroxides are formed.[83] Thus, it is thought that an equilibrium exists between the pentahydroxide, $[UO_2(OH)_5]^{3-}$, and the tetrahydroxide, $[UO_2(OH)_4]^{2-}$, with the pentahydroxide being the dominant species. Hence, it is likely that the experimental value cited in Table 1 refers to the pentahydroxide, $[UO_2(OH)_5]^{3-}$, or a mixture of $[UO_2(OH)_4]^{2-}$ and $[UO_2(OH)_5]^{3-}$, rather than to the tetrahydroxide. I have not studied the pentahydroxide here. Test calculations show that its high negative charge will result in optimized bond lengths that are far too long. Given the well-known geometry dependence of calculated NMR parameters,[1] NMR shielding calculations on this system would then be meaningless if they were based on such an optimized gas-phase geometry.

I have further tried to understand the systematic errors in the ^{17}O NMR by studying the geometry dependence of the shielding that were also discussed in Part 1. Here, I have chosen the uranyl water complex as a representative example. The complete data have been included in the Supporting Information. Taking finite difference derivatives, a shielding gradient for the uranyl oxygen of about −2485 ppm/Å was found for changes of the uranyl bond length, and 251 ppm/Å for changes in the water bond distance. Comparing optimized and experimental structures, one can see that the optimized water distance is too large by about 0.1 Å as compared to experiment,[88−90] whereas the uranyl distance is too short by 0.01[89] or 0.03 Å,[90] respectively, depending on the particular experimental investigation. Thus, the geometry errors in the uranyl distances would contribute some −25 to −75 ppm to the error in the shieldings. This would mean up to +25 to 75 ppm for the chemical shift, unless part of the error cancels out. Likewise, the error in the equatorial ligand bond lengths would yield changes of some 25 ppm in the shieldings, corresponding to a maximum correction of about −25 ppm in the chemical shifts. Overall, the geometry errors appear not to be the dominating error source for the uranyl oxygen chemical shifts.

Experimental NMR data is also available for some other nuclei apart from the uranyl oxygens. For instance, for the hydroxide system, a second ^{17}O chemical shift signal has been observed.[83] However, this particular signal has been assigned to a weighted average between bound OH^- and free H_2O; it has been shown experimentally that there is a fast exchange between the solvent and the bound hydroxide groups. Such exchange processes cannot be modeled with the current theoretical tools that principally consider an isolated molecule only.

Additional experimental data is available for the uranyl tricarbonate anion, $[UO_2(CO_3)_3]^{4-}$. In this case, average ^{13}C and ^{17}O chemical shifts have been measured for the equatorial carbonate ligands (Table 2).[82] The experimental average shielding value for the ^{17}O and ^{13}C carbonate shieldings, 66 and 18.4 ppm, respectively, should be compared with calculated values of 11.6 and 0.4 ppm, respectively (ZORA spin−orbit). Spin−orbit effects are seen to have a modest influence only. Again, solvation effects and exchange processes are expected to be important experimentally but have been neglected in the calculations. Other error sources could include the model for the XC functional of DFT (part 1) and the optimized geometries.

(B) Methoxy Derivatives of UF_6, $UF_{6-n}(OCH_3)_n$: ^{19}F NMR. In the first paper of the series,[39] the ^{19}F NMR chemical shifts in mixed uranium chloride fluorides, $UF_{6-n}Cl_n$, were discussed. Here, I will continue and extend these discussions by considering the fluorine NMR chemical shifts in the related organometallic derivatives of UF_6, $UF_{6-n}(OCH_3)_n$, $n = 1-5$. The calculated ^{19}F NMR chemical shifts for these compounds have been collected in Table 3, where they are also compared to experimental data.[91] Besides the measurements by Cuellar and Marks,[91] there is additional NMR data for the first member of the series, UF_5OCH_3. Thus, Vergamini[92] reports ^{19}F NMR chemical shifts for UF_5OCH_3 taken relative to UF_6 ($CFCl_3$ solution). His numbers of $\delta(^{19}F, V) = 56.3 \pm 0.3$ ppm and $\delta(^{19}F, X_4) = 117 \pm 0.5$ ppm should be compared to the measurements of Cuellar and Marks[91] for the same solvent, 58.1 and 121.1 ppm, respectively (Table 3). Thus, the two sets of experiments agree well with one another, as long as the same solvent is used.

Cuellar and Marks[91] have performed their experiments in $CFCl_3$ and CH_2Cl_2 solutions. Both sets of experiments have been included in Table 3, and one should notice solvent effects that are considerable. The dependence of the measured ^{19}F chemical shifts on the solvent grows with the number of methoxy ligands and reaches a maximum of 58 ppm for $UF(OCH_3)_5$ (Table 3). Such a strong dependence is an indication that gas-to-liquid shifts should not be small either.

(88) Hay, P. J.; Martin, R. L.; Schreckenbach, G. *J. Phys. Chem. A* **2000**, *104*, 6259−6270.
(89) Allen, P. G.; Bucher, J. J.; Shuh, D. K.; Edelstein, N. M.; Reich, T. *Inorg. Chem.* **1997**, *36*, 4676−4683.
(90) Wahlgren, U.; Moll, H.; Grenthe, I.; Schimmelpfennig, B.; Maron, L.; Vallet, V.; Gropen, O. *J. Phys. Chem. A* **1999**, *103*, 8257−8264.
(91) Cuellar, E. A.; Marks, T. J. *Inorg. Chem.* **1981**, *20*, 2129−2137.
(92) Vergamini *J. Chem. Soc., Chem. Commun.* **1979**, 54−55.

Table 3. ^{19}F Chemical Shifts (Pauli spin−Orbit, ZORA Spin−Orbit, and Experiment[a]) in Methoxy Compounds $UF_{6-n}(OCH_3)_n$, $n = 0-5$ (numbers in ppm)

		^{19}F chemical shift			
		calculated[c]		experiment[a]	
molecule	site[b]	Pauli	ZORA	CH_2Cl_2 solutions	$CFCl_3$ solutions
UF_6		846.5	831.0	766.5	764.3
$UF_5(OCH_3)$	V	763.9	747.2	690.3	706.2
	X	748.6	736.4	627.2	643.5
trans-$UF_4(OCH_3)_2$		670.4	660.3	512.5	542.8
cis-$UF_4(OCH_3)_2$	V	681.9	670.3	578.1	
	X	673.9	663.2	[512.5][d]	
mer-$UF_3(OCH_3)_3$	V	612.7	606.3	486.5	526.7
	X	597.1	592.9	418.2	459.6
fac-$UF_3(OCH_3)_3$		610.7	604.5	483.0	
trans-$UF_2(OCH_3)_4$			539.6	337.8	385.5
cis-$UF_2(OCH_3)_4$			559.2	397.4	453.5
$UF(OCH_3)_5$			509.4	330.5	388.2

[a] Reference 91; estimated experimental uncertainties of ±0.2 ppm (CH_2Cl_2 solutions) and ±0.3 ppm ($CFCl_3$ solutions), respectively. [b] V, fluoride ligand trans to a methoxy ligand; X, fluoride ligand trans to a fluoride ligand. [c] Average values. The chemical shifts are based on calculated ^{19}F shielding values for $CFCl_3$ of $\sigma(^{19}F, CFCl_3, \text{ZORA spin−orbit}) = 130.7$ ppm and $\sigma(^{19}F, CFCl_3, \text{Pauli spin−orbit}) = 130.6$ ppm, respectively; cf. eq 1. [d] Experimental number based on *assumed* degeneracy with *trans*-$UF_4(OCH_3)_2$.

This will limit the agreement between theory and experiment, since any kind of medium effects have been neglected for the former.

Given these intrinsic limitations, the agreement between theory and experiment is reasonable. In particular, the Pauli and ZORA calculations reproduce experimental trends qualitatively. These trends include, for instance, the decreasing chemical shift along the series or the relative ordering of the V and X sites within a molecule [$UF_5(OCH_3)$, *cis*-$UF_4(OCH_3)_2$, *mer*-$UF_3(OCH_3)_3$, but also *cis*- versus *trans*-$UF_2(OCH_3)_4$]. This is interesting since, for the related fluoride chlorides $UF_{6-n}Cl_n$, similar qualitative trends were consistently missed by the calculations, (Part 1). The qualitative agreement between theory and experiment is also evident from Figure 1. In this figure, I have plotted the calculated (ZORA spin−orbit) ^{19}F NMR chemical shifts as a function of the number of fluorine ligands cis to the resonant nucleus. The chemical shifts fall on two smooth curves, one (the upper one) for resonating fluorine nuclei that are situated trans to another fluorine and one (the lower one) for those nuclei that are situated trans to a methoxy ligand. The theoretical graph is in good qualitative agreement with the corresponding experimental plot.[91]

While qualitative agreement between theory and experiment has been achieved, the quantitative agreement is not as good; the deviations are still fairly large. They are on the same order as those that had been found in the first paper of the series for the $UF_{6-n}Cl_n$ series. This time, the chemical shift is systematically overestimated by either method. This might be partly due to the calculated ^{19}F shielding values for the reference compound ($CFCl_3$) or to the choice of XC functional; see also Part 1. Nevertheless, the source of these systematic errors is not entirely clear at this point. The calculated Pauli chemical shifts are consistently larger than their ZORA counterparts, making ZORA the more accurate

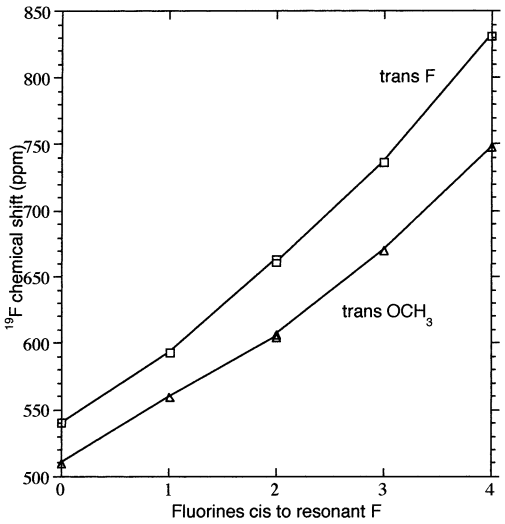

Figure 1. Plot of the calculated chemical shifts $\delta(^{19}F)$ versus the number of fluorines cis to the resonant F in the series $UF_{6-n}(OCH_3)_n$, $n = 0-5$ (ZORA spin−orbit calculations). The upper curve (squares) refers to fluorine atoms situated trans to another fluorine, and the lower curve (triangles) refers to fluorine atoms situated cis to another fluorine.

approach in this case. Certainly, the mentioned solvation effects will be important as well. The lack of quantitative agreement is also evident when comparing Figure 1 to the corresponding experimental plot.[91] Thus, the two experimental curves are almost coinciding on the left-hand side of the graph.[91] This is not the case for the theoretical chemical shifts (Figure 1).

I have attempted to investigate the various potential sources for the systematic error in the calculated ^{19}F chemical shifts. To test the geometry dependence of the fluorine NMR—and thus the influence of errors in the optimized geometries—I have first calculated the shieldings in $UF_5(OCH_3)$ for various displacements of the CH_3 group. The data are given in the Supporting Information; such distortions have hardly any influence on the calculated fluorine NMR. Next, I have tested the influence of the fluorine position by varying the U−F bond distances in UF_6. The data are given in the Supporting Information also. One can see that the shielding gradient for the ^{19}F NMR amounts to some −1800 ppm/Å or so near the experimental bond distance of 1.999 Å [93,94] (ZORA spin−orbit calculations). Given that the optimized bond length is too long by about 0.02−0.03 Å,[74] I should have calculated ^{19}F shieldings that are too negative as compared to experiment. Thus, part of the systematic error in the calculated ^{19}F chemical shifts could be due to the errors in the optimized geometries.

(C) Methoxy Derivatives of UF_6, $UF_{6-n}(OCH_3)_n$: ^{1}H NMR, Other Nuclei. I have further studied the proton NMR of the mixed methoxyuranium(VI) fluorides, $UF_{6-n}(OCH_3)_n$, $n = 1-5$. The results have been collected in Table 4 and Figure 2, where the calculated and experimental proton chemical shifts are compared. On the theoretical side, I took the average over the calculated chemical shifts for the different protons to enable a comparison with experiment.

(93) Weinstock, B.; Goodman, G. L. *Adv. Chem. Phys.* **1965**, *9*, 169.
(94) Seip, H. M. *Acta Chem. Scand.* **1965**, *20*, 2698.

Table 4. ^{1}H Absolute Shieldings and Chemical Shifts (Pauli Spin−Orbit, ZORA Spin−Orbit, and Experiment[a]) in Methoxy Compounds $UF_{6-n}(OCH_3)_n$, $n = 1-5$ (numbers in ppm)

				^{1}H chemical shift δ				
		calculated shielding σ[c]			calculated[c,d] (Pauli)		calculated[c,d] (ZORA)	
molecule	site[b]	Pauli	ZORA	experiment[a]	value	error[e]	value	error[e]
$UF_5(OCH_3)$		19.17	18.39	12.13	11.76	−0.37	12.48	0.35
trans-$UF_4(OCH_3)_2$		21.31	20.69	9.29	9.62	0.33	10.18	0.89
cis-$UF_4(OCH_3)_2$		20.68	19.83	10.73	10.25	−0.48	11.04	0.31
mer-$UF_3(OCH_3)_3$	A	21.96	21.25	8.79	8.97	0.18	9.62	0.83
	M	21.21	20.43	9.57	9.72	0.15	10.44	0.87
fac-$UF_3(OCH_3)_3$		21.52	20.57	9.50	9.41	−0.09	10.30	0.80
trans-$UF_2(OCH_3)_4$			21.87	8.32			9.00	0.68
cis-$UF_2(OCH_3)_4$	A		22.14	8.42			8.73	0.31
	M		21.29	9.01			9.58	0.57
$UF(OCH_3)_5$	A		22.39	8.02			8.48	0.46
	M		21.89	8.37			8.98	0.61

[a] Reference 91. $CD_2Cl_2/CDCl_3$ solution; estimated experimental uncertainty of ±0.04 ppm. [b] A, methoxy ligand trans to a methoxy ligand; M, methoxy ligand trans to a fluoride ligand. [c] Average over the different hydrogens. [d] Chemical shift based on calculated ^{1}H shielding value for TMS of σ(^{1}H, TMS, ZORA spin−orbit) = 30.87 ppm and σ(^{1}H, TMS, Pauli spin−orbit) = 30.93 ppm, respectively. I have employed the experimental structure for TMS;[71] see the text and the discussion in Part 1. [e] Error: δ(calculated) − δ(experimental).

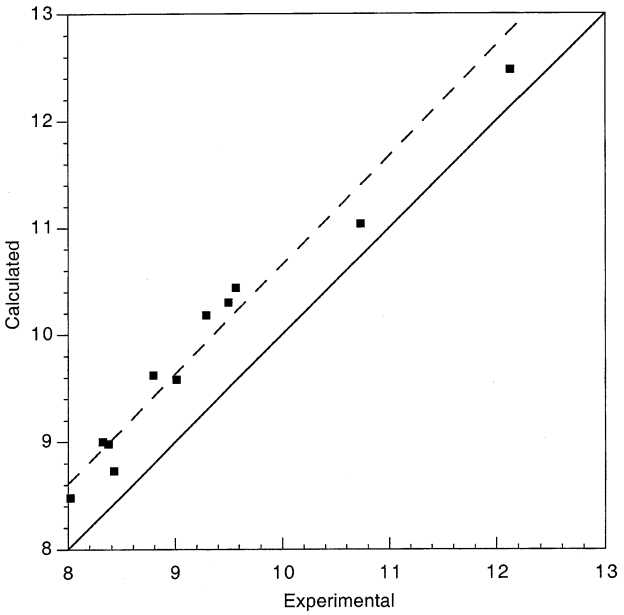

Figure 2. Calculated (ZORA spin−orbit) and experimental[91] ^{1}H NMR chemical shifts in methoxy compounds $UF_{6-n}(OCH_3)_n$, $n = 1-5$ (ppm). Marked in the figure are a line corresponding to perfect agreement between theory and experiment (solid line) and another line that is shifted from the first one by 0.61 ppm, i.e., the average deviation between theory and experiment (broken line).

As has been shown in the first paper of the series already, these are cases where the inclusion of spin−orbit is essential for quantitatively and even qualitatively correct results. Spin−orbit chemical shifts of about 7 ppm were found for the first member of the series, $UF_5(OCH_3)$ (Part 1). The effect of spin−orbit on the calculated ^{1}H shieldings and chemical shifts is similarly large for the other members of the series.

Excellent agreement is found between calculated and experimental proton chemical shifts for this series of compounds. All experimental trends have been reproduced nicely by the calculations (Table 4). This is true for both the Pauli and ZORA approaches. For instance, the relative ordering of inequivalent sites within one molecule has been reproduced in all cases [*mer*-$UF_3(OCH_3)_3$, *cis*-$UF_2(OCH_3)_4$, $UF(OCH_3)_5$]. Likewise, trends along the series are also reproduced by the Pauli and ZORA spin−orbit calculations. As has been discussed in Part 1, the proton NMR in these compounds is a rare example where Pauli calculations give better agreement with experiment than ZORA. Despite this observation, the conclusion was that ZORA is still the more accurate method of the two on an overall basis. Hence, I will concentrate more on the ZORA calculations in the following discussions.

The average deviation between theory (ZORA) and experiment is 0.61 ppm, if one simply takes the average of the errors listed in Table 4. The same average deviation, 0.61 ppm, results from a weighted average where the degeneracy has been taken into account.[95] The ZORA calculations overestimate the chemical shift in all cases (Figure 2). Part of this error might be the due to the calculated shielding of the reference compound, tetramethylsilane (TMS) (Part 1). Thus, it appears to be justified to improve the agreement with the experiment by reducing all calculated shieldings by 0.61 ppm (Figure 2). Doing this reduces the average absolute deviation to 0.19 ppm, and the weighted average absolute deviation to 0.18 ppm.

The remaining, small error may be due to a number of reasons, besides systematic inadequacies of the theoretical tools. In my calculations, again solvation effects have been neglected. Furthermore, no attempt has been made to account for rovibrational effects.[1] Such effects are known to be particularly large for the proton NMR, due to the small nuclear weight and resulting large vibrational amplitudes of the hydrogen nucleus.[96] Finally, only one conformation per molecule has been studied, not necessarily the lowest energy conformation in each case.[74] In this way, the entire conformational space that is accessible to the molecules in a solution has not been accounted for. This is particularly true for the lower members of the series with $n > 1$.

NMR shieldings have been calculated also for the other nuclei in the $UF_{6-n}(OCH_3)_n$ series (^{13}C, ^{17}O). However, no

(95) For instance, 12 protons contribute to the A_4 signal of $UF(OCH_3)_5$ but only three protons to the M site.

(96) Ruud, K.; Åstrand, P.-O.; Taylor, P. *J. Am. Chem. Soc.* **2001**, *123*, 4826−4833.

Table 5. Predicted ^{235}U NMR Absolute Shieldings and Chemical Shifts[a] (ppm) for Different Computational Approaches

	Pauli scalar		Pauli spin−orbit		ZORA scalar		ZORA spin−orbit	
molecule	abs shielding	chemical shift	abs shielding	chemical shift	abs shielding	chemical shift	abs shielding	chemical shift
UF_6	**−837**	0	**−1126.8**	0	**−6703**	0	**678**	0
UF_5Cl	**−3194**	2357	**−3457.7**	2331	**−9178**	2475	**−1934**	2612
cis-UF_4Cl_2	**−5321**	4484	**−5559.1**	4432	**−11391**	4689	**−4206**	4884
trans-UF_4Cl_2	**−5796**	4959	**−6177.8**	5051	**−11702**	4999	**−4589**	5268
fac-UF_3Cl_3	**−7291**	6454	**−7535.1**	6408	**−13429**	6726	**−6239**	6918
mer-UF_3Cl_3	**−7550**	6713	**−7883.6**	6757	**−13651**	6948	**−6541**	7219
cis-UF_2Cl_4	**−9245**	8408	**−9572**	8445	**−15545**	8843	**−8388**	9016
trans-UF_2Cl_4	**−9360**	8523	**−9760.3**	8634	**−15703**	9000	**−8631**	9309
$UFCl_5$	**−10796**	9959	**−11179.1**	10052	**−17445**	10743	**−10275**	10954
UCl_6	**−12042**	11205	**−12466.8**	11340	**−19286**	12583	**−12057**	12735
$UF_5(OCH_3)$	**−225**	−612	**−2427.9**	1301	**−7961**	1258	**−646**	1324
cis-$UF_4(OCH_3)_2$	**−3126**	2289	**−3171**	2044	**−8671**	1968	**−1315**	1993
trans-$UF_4(OCH_3)_2$	**−3380**	2543	**−3570**	2443	**−9003**	2300	**−1596**	2274
fac-$UF_3(OCH_3)_3$	**−3986**	3149	**−3942**	2816	**−9499**	2796	**−2315**	2993
mer-$UF_3(OCH_3)_3$	**−4121**	3284	**−4164**	3037	**−9644**	2942	**−2236**	2914
cis-$UF_2(OCH_3)_4$							**−2660**	3338
trans-$UF_2(OCH_3)_4$							**−2739**	3417
$UF(OCH_3)_5$							**−3095**	3773
$[UO_2F_4]^{2-}$	**1364.7**	−2201	**+1139**	−2266	**−2848**	−3854	**+5207**	−4528
$[UO_2Cl_4]^{2-}$	**−81.7**	−755	**−418**	−709	**−4498**	−2204	**+3954**	−3276
$[UO_2(OH)_4]^{2-}$	**−808**	−29	**−1015.6**	−111	**−5471**	−1231	**+2581**	−1903
$[UO_2(CO_3)_3]^{4-}$	**−1020**	183	**−1338.1**	211	**−6129**	−574	**+2282**	−1604
$[UO_2(H_2O)_5]^{2+}$ (D_5)	**3330**	−4167	**+3399**	−4526	**−82**	−6621	**+8954**	−8276
$[UO_2(H_2O)_5]^{2+}$ (D_{5h})[b]	**3283**	−4120	**+3355**	−4481	**−145**	−6558	**+8855**	−8176

[a] Chemical shifts taken relative to UF_6, as calculated at the respective level of theory. [b] The optimized ground-state structure has D_5 symmetry at the given level of theory. The idealized D_{5h} structure possesses five imaginary frequencies and has a higher energy.

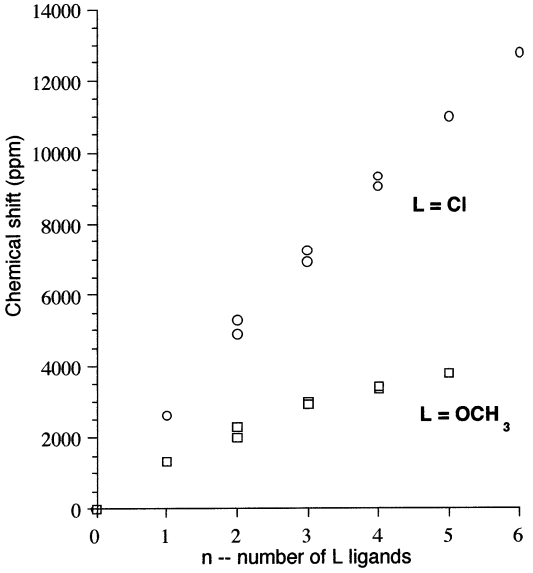

Figure 3. Calculated ^{235}U chemical shifts in $UF_{6-n}L_n$ compounds as a function of *n*.

comprehensive experimental data exists for these nuclei. I have included the calculated shieldings for future reference as part of the Supporting Information.

(D) Uranium (^{235}U) NMR Shieldings and Chemical Shifts. Theoretical methods have been used also to calculate actinide metal (^{235}U) NMR shieldings. The results are shown in Table 5. In addition, part of the data is presented in Figure 3. The ability to calculate NMR shieldings and chemical shift for a heavy element like uranium is a particular strength of the relativistic DFT-ZORA and DFT-QR methods.

Only once has an NMR signal of an actinide nucleus been observed, namely for UF_6.[51] Hence, ^{235}U relative chemical shifts (or any other actinide shifts) have not yet been measured, due to an unfavorable signal-to-noise ratio combined with the large chemical shift range and the radioactivity of the actinides. It is hoped that the present calculations might help to guide future experiments, by narrowing down the magnetic field ranges that have to be scanned for a signal. In preliminary studies,[41] a ^{235}U chemical shift range of at least 12 000 ppm was predicted. The current studies include a more comprehensive set of molecules, and the predicted shielding (chemical shift) range is now nearly doubled (Table 5). Thus, a rather large range of at least 21 000 ppm for the 23 molecules studied was predicted (ZORA spin−orbit calculations).

Calculated ^{235}U chemical shifts are also included in Table 5. As of yet, there is no standard experimental reference compound for the ^{235}U nucleus. UF_6 has been selected for this purpose. UF_6 was chosen because it is a relatively small and very well characterized molecule. Indeed, as has been discussed above, it is the only case where a ^{235}U NMR spectrum has ever been detected.[51] Furthermore, it is highly symmetric, making it more accessible than other molecules for both calculations and measurements. (Note that ^{235}U is a quadrupolar nucleus.) The uranyl pentaaquo complex, $[UO_2(H_2O)_5]^{2+}$, could perhaps be used as an alternative to UF_6. It has the highest shielding (lowest chemical shift) of all the molecules in Table 5. Thus, using it as the reference compound would lead to all positive uranium chemical shifts for the set of molecules studied.

The relativistic ZORA spin−orbit approach was applied to all molecules in Table 5. In addition, calculations were performed on most of the molecules using other levels of theory. Comparing scalar and spin−orbit ZORA calculations, very large spin−orbit relativistic effects were noted. Some parts of these effects cancel out in relative chemical shifts.

This cancellation is a hint that these are core-type relativistic effects. As has been discussed in section 2, such core-type spin−orbit effects arise because the spin−orbit-induced spin polarization is picked up by the core-type s-orbitals ($1s_{1/2}$, $2s_{1/2}$, etc.) at the heavy uranium nucleus itself. The core-type spin−orbit should also be responsible for (part of) the large difference, or constant offset, between the calculated Pauli spin−orbit and ZORA spin−orbit absolute shieldings. While some scalar relativistic effects of the core are included approximately in the Pauli method[14] (see also below), core-type spin−orbit effects are not. They are, however, included into the all-electron ZORA calculations.

Interestingly, an even larger difference is observed between Pauli and ZORA shieldings that were calculated without spin−orbit effects, i.e., in the scalar relativistic approximation (Table 5). Again, a large part of these differences cancels out in relative chemical shifts. These differences, too, are due to core effects. One can understand them as follows. First, the core part of the basis is of double-ζ quality in ZORA calculations but only single-ζ in the Pauli case (section 3 and Part 1). Surely, this will have a large influence on the core−core and core−valence parts of the paramagnetic shielding, given the large extent of the uranium core.[97] Second, let us recall that there are three distinct scalar shielding contributions of the core.[59] These are paramagnetic core−core and core−valence contributions and the diamagnetic shielding of the core density. The last two contributions are accounted for by either method, exactly through ZORA all-electron calculations and approximately in the (Pauli) frozen-core case. However, core−core contributions, resulting from the paramagnetic coupling between pairs of occupied core MOs, are neglected in the frozen-core approximation, i.e., in Pauli calculations.[59] Again, given the large uranium core, these contributions will be sizable. Together with the basis set effects, they should be responsible for a good part of the difference between ZORA and Pauli scalar shieldings, namely the piece that cancels out in relative chemical shifts. It is noteworthy that the core-type spin−orbit shielding compensates for part of the large difference between the scalar Pauli and ZORA methods.

Let us come back to the spin−orbit effects on the ^{235}U NMR. Valence effects that survive in relative chemical shifts are seen to be modest for the given set of molecules (Table 5). It is, however, not possible to neglect them either. In particular, they do not necessarily have the same sign, cf. the $UF_{6-n}L_n$ complexes versus the uranyl complexes. Large spin−orbit effects on the metal chemical shifts are expected for molecules containing heavy ligand atoms.[31] Here, only systems with comparatively light ligand nuclei were studied. The heaviest ligand nucleus in the studies is the chlorine atom. Comparing scalar and spin−orbit ZORA calculations, a relatively large spin−orbit chemical shift of about 600 ppm was noticed for the largest number of chlorine ligands (UCl_6).

Comparing the calculated chemical shifts from the Pauli and ZORA methods, one can note that qualitative trends are predicted similarly by either method. However, quantitative differences remain in the absolute numbers. They reach 1400 ppm for UCl_6 and as much as 3750 ppm for $[UO_2(H_2O)_5]^{2+}$ (Table 5). The lack of experimental data prevents any final judgment on the accuracy of either method as applied to the calculation of ^{235}U NMR chemical shifts. Nevertheless, the well-known theoretical shortcomings of the Pauli approach (numerical instability, limitations to the basis sets) lead me to believe that the ZORA spin−orbit ^{235}U chemical shifts are more accurate than their Pauli counterparts. This is supported by the results for the ligand nuclei (see above and Part 1) and for other systems.[31−33,97] Indeed, I would like to go even further and conclude that the Pauli approach appears to be at or beyond its limits for the NMR of the very heavy actinide nuclei. This conclusion is based, in particular, on the large differences between Pauli and ZORA for the uranyl systems (Table 5). For one of them ($[UO_2(CO_3)_3]^{4-}$), the two methods are in disagreement even over the sign of the chemical shift. The conclusion is supported by the fact that a number of important shielding contributions are neglected in the Pauli case. This concerns, in particular, the quality of the basis in the core region, the core-type spin−orbit contributions, and certain core−core paramagnetic interactions, as has been discussed in detail above. Obviously, these are primarily core effects. Nevertheless, it is unlikely that they would have no valence effect at all and would cancel out completely in relative chemical shifts.

(E) Factors Influencing Calculated Chemical Shifts. The Example of ^{235}U NMR in the $UF_{6-n}L_n$ Series (L = Cl, OCH_3). As has been pointed out above, the DFT-GIAO approach allows for a detailed analysis of the calculated shieldings and chemical shifts in terms of the electronic structure (section 4). In the following, I intend to apply the analysis tools that are available in this method to the calculated ^{235}U shieldings and chemical shifts. From now on, I discuss mostly only ZORA spin−orbit calculations.

As a start, the contributions to the calculated ^{235}U shieldings are collected in Table 6. According to eq 2, there are three distinct contributions to the calculated shielding (chemical shift). The diamagnetic shielding, σ^d, does not vary by more than about 20 ppm. This change is really negligible, given a total calculated shielding range of over 21 000 ppm. Hence, σ^d has no influence on the relative chemical shifts. This result is readily understandable from the fact that the core MOs, $1s_{1/2}$ in particular, contribute by far the largest part of the diamagnetic shielding. That is a consequence of the localized nature of the NMR shielding/chemical shift (cf. eq 4). Such core effects are largely independent from the chemical environment of the uranium nucleus. They cancel out in relative chemical shifts. Similar conclusions have been drawn before for other nuclei (e.g., refs 5, 15, 17, 30−32).

The spin−orbit shielding, σ^{so} of eq 6, has already been discussed in the previous section, where it was found that it has a large influence on the calculated absolute shieldings. Furthermore, it was observed that it has, for the given set of molecules, a modest although not negligible influence on the chemical shifts. This conclusion is supported by the numbers in Table 6. One can see that σ^{so} varies within a

(97) Bouten, R.; Baerends, E. J.; van Lenthe, E.; Visscher, L.; Schreckenbach, G.; Ziegler, T. *J. Phys. Chem. A* **2000**, *104*, 5600−5611.

Table 6. Contributions to the ^{235}U Shieldings (Eqs 2 and 3) (ZORA Spin−Orbit)

	shieldings, σ (ppm)				
				σ^{p}	
molecule	σ (total)	σ^{d}	σ^{so}	total	$\sigma^{p,oc-vir}$
UF_6	678	11 610	7 964	−18 896	−15 380
UF_5Cl	−1 934	11 615	7 758	−21 306	−18 180
cis-UF_4Cl_2	−4 206	11 619	7 624	−23 449	−20 628
trans-UF_4Cl_2	−4 589	11 617	7 506	−23 713	−21 488
fac-UF_3Cl_3	−6 239	11 623	7 548	−25 411	−22 742
mer-UF_3Cl_3	−6 541	11 621	7 436	−25 598	−23 596
cis-UF_2Cl_4	−8 388	11 625	7 402	−27 415	−25 471
trans-UF_2Cl_4	−8 631	11 623	7 297	−27 551	−26 286
$UFCl_5$	−10 275	11 627	7 308	−29 211	−27 888
UCl_6	−12 057	11 629	7 248	−30 935	−30 148
$UF_5(OCH_3)$	−646	11 612	7 819	−20 077	−16 808
cis-$UF_4(OCH_3)_2$	−1 315	11 613	7 780	−20 708	−17 832
trans-$UF_4(OCH_3)_2$	−1 596	11 613	7 840	−21 049	−18 526
fac-$UF_3(OCH_3)_3$	−2 315	11 614	7 583	−21 512	−19 023
mer-$UF_3(OCH_3)_3$	−2 236	11 614	7 783	−21 633	−19 429
cis-$UF_2(OCH_3)_4$	−2 660	11 614	7 712	−21 986	−20 181
trans-$UF_2(OCH_3)_4$	−2 739	11 614	7 827	−22 180	−20 617
$UF(OCH_3)_5$	−3 095	11 615	7 779	−22 489	−21 277
$[UO_2F_4]^{2-}$	5 207	11 618	8 285	−14 696	−13 545
$[UO_2Cl_4]^{2-}$	3 954	11 621	8 371	−16 038	−15 644
$[UO_2(OH)_4]^{2-}$	2 581	11 616	8 163	−17 199	−17 355
$[UO_2(CO_3)_3]^{4-}$	2 282	11 618	8 235	−17 571	−17 858
$[UO_2(H_2O)_5]^{2+}$ (D_5)	8 954	11 613	8 775	−11 434	−13 016

range of some 1500 ppm, about 6.5% of the total calculated chemical shift range. The spin−orbit shielding is expected to become much more prominent for complexes where the uranium atom is bound to ligands that contain heavy atoms (e.g., UX_6, X = Br, I, or $UF_{6-n}(OTeF_5)_n$,[98] $n = 0-6$) or also for systems containing more than one actinide nucleus. The spin−orbit shielding σ^{so} could well be the most important factor in such cases.

For the given molecules, the largest contribution to the calculated ^{235}U shieldings and chemical shifts is due to the paramagnetic shielding, σ^{p} (Table 6). According to eq 3 and the accompanying discussion, the leading contribution to σ^{p} is one that couples occupied and virtual molecular orbitals, $\sigma^{p,oc-vir}$. This follows also from Table 6, where I have included the calculated values of $\sigma^{p,oc-vir}$. From the table one can note that the remaining (occupied−occupied) contribution to σ^{p} is neither small nor negligible, and it can have either sign. Nevertheless, $\sigma^{p,oc-vir}$ is responsible for the largest part of the paramagnetic shielding, as well as for the various trends in the shieldings and chemical shifts. For a qualitative discussion, one can focus on this contribution.

In the following, I wish to use the analysis tools of the DFT-GIAO method (eqs 3−5) to make the connection between σ^{p} and the calculated electronic structure. I have chosen the UF_6 derivatives $UF_{6-n}L_n$ as a representative example. For these molecules, I would like to discuss and rationalize the chemical shift trend that is apparent in Table 5 and Figure 3. Trends in the electronic structure along the chloride series (L = Cl) have been discussed in a separate publication.[74] I intend to use these results for the following discussion. From Figure 3 one can note that the calculated ^{235}U chemical shift increases for increasing *n*, more so for the chloride fluorides than for the methoxy series. It follows from Table 6 that the trend is mostly due to an increase in absolute terms of the (negative) paramagnetic shielding contribution σ^{p} that, in turn, is dominated by $\sigma^{p,oc-vir}$ (eq 3). The occupied−virtual shielding $\sigma^{p,oc-vir}$ can be broken down into contributions from individual pairs of occupied and virtual MOs (eqs 3 and 5). A direct inspection of the calculations shows that the largest individual contributions involve, in each case, the seven lowest virtual MOs. In a simple ionic picture, these would be the 5f orbitals at the uranium center. In a more realistic bonding picture, these MOs are still mostly 5f orbitals but have considerable antibonding ligand contributions as well.[74] The only exception is, in each case, the lowest unoccupied MO (LUMO). It is a pure f_{xyz} orbital, and its symmetry properties prevent any mixing with the ligand MOs. Earlier studies[74] showed that the percentage of f-character of the remaining six 5f type virtuals decreases along the fluoride chloride series, from 82.0% for UF_6 to 78.5% for UCl_6.[99] This decrease in virtual f-character will be accompanied by an increase in 5f-character for the corresponding occupied MOs.

One can conclude that, at least qualitatively, the trends in the occupied−virtual shielding, $\sigma^{p,oc-vir}$, the total paramagnetic shielding, σ^{p}, as well as the total shielding and chemical shift are dominated by metal-based occupied−virtual f-to-f-transitions. In principle, also metal-based d-to-d- and p-to-p-transitions could contribute. An inspection of the calculations shows that this is, indeed, the case. However, the corresponding occupied MOs are typically much lower in energy than the f-type MOs, and the virtuals are higher in energy. Overall, the occupied−virtual separation is much larger for the d-to-d- and p-to-p-couplings than for the f-to-f-transitions. According to eq 5, the magnitude of an occupied−virtual shielding contribution is inversely proportional to the energy gap. The large gap explains why the d- and p-based transitions contribute much less to the paramagnetic shielding than their 5f counterparts.

At that point, I wish to come back to the trends in the calculated ^{235}U shielding along the $UF_{6-n}L_n$ series (Figure 3 and Table 5). It was found that the shielding is dominated by occupied−virtual 5f-type couplings. How do these paramagnetic couplings change along the series?

To answer this question, one can again resort to earlier investigations of the fluoride chloride molecules.[74] There, an average position of the occupied f-containing MOs was calculated. This was done by taking an average over the MO energies of occupied MOs, using the percentage f-character and degeneracy as weighing factors. Similarly, the weighted average was taken over the seven lowest virtual MOs. These results from earlier study are summarized in Figure 4.[74] Some of the data is given as Supporting Information also.

The results in Figure 4 are based on scalar relativistic calculations; i.e., spin−orbit effects have been neglected. Earlier, the role of spin−orbit effects were discussed, the spin−orbit shielding σ^{so} (eqs 2 and 6) in particular. Here, scalar relativistic calculations are sufficient for the given

(98) Seppelt, K. *Chem. Ber.* **1976**, *109*, 1046−1052.

(99) Data taken from ref 74. ADF-based scalar relativistic QR-PW91 calculations; percentage f-character was based on AO coefficients.

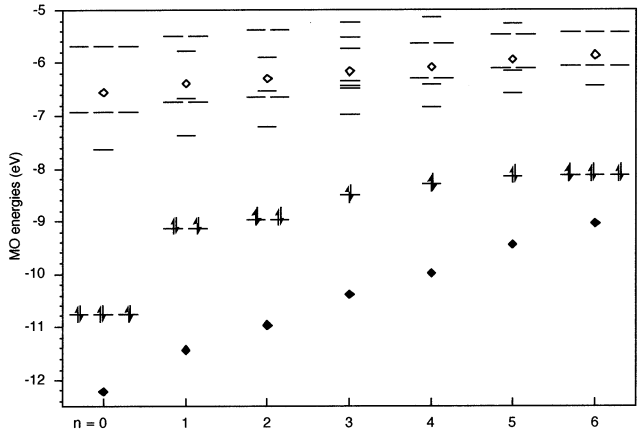

Figure 4. $UF_{6-n}Cl_n$ molecules, $n = 0-6$: Shown for each molecule are the HOMO (marked schematically by its occupation), the seven lowest virtual MOs (the U 5f orbitals), the weighted average position of occupied MOs with U 5f-character (solid diamonds), and the weighted average of the U 5f-orbitals, i.e., the seven lowest virtual MOs (open diamond); see the text. (Data taken from ref 74.)

purpose, since the spin−orbit-induced splitting of certain degenerate shells will, to first order, cancel out in eq 5 and related expressions. (For instance, recall that the three degenerate orbitals of an atomic p shell are split into one lower $p_{1/2}$ orbital and two degenerate $p_{3/2}$ orbitals of higher energy with the average being at the position of the scalar relativistic p orbital.)

It follows from Figure 4 that the average position of occupied MOs with U 5f character and the average position of the seven lowest virtuals (the U 5f orbitals) increase monotonically with growing n.[74] The increase of the occupied average (solid diamonds in Figure 4) is greater than that of the virtuals (open diamonds in the figure). Consequently, the gap between the two is decreasing considerably along the series. On the side, recall that no similar trend exists for the HOMO−LUMO gap.[74] Indeed, the first member of the series, UF_6, has a HOMO−LUMO gap that is almost twice as large as for any other molecule.

The change in occupied virtual f-to-f-separation is the major factor responsible for the trends in the ^{235}U NMR shielding (Table 6). According to eq 5, the paramagnetic shieldings $\sigma^{p,oc-vir}$ and σ^{p} are inversely proportional to the energy separation between the occupied and virtual MOs involved. In the given case, these are occupied and virtual MOs that couple primarily through their 5f contribution at the uranium center, as has been discussed above. The gap between the average positions of the 5f containing occupied and virtual MOs (Figure 4) can serve as a measure for the energy separation (eq 5). One notes from Table 6 that $\sigma^{p,oc-vir}$ is more than doubled in going from UF_6 to UCl_6. At the same time, the occupied−virtual gap decreases by a factor of 1.8, from 5.652 to 3.175 eV.[74] Thus, there is an almost quantitative correlation between the f-to-f-occupied−virtual gap and the paramagnetic shielding.

The degree of quantitative agreement can be improved even further if one considers also the f-character of the occupied and virtual MOs. As has been mentioned already, the f-character of the virtuals decreases along the series. This is accompanied by a corresponding increase in f-character of the 5f-containing occupied MOs, from 18.0% for UF_6 to 21.5% for UCl_6.[74] This, in turn, will lead to a better overlap (increased magnetic interaction) between the occupied and virtual MOs involved (eqs 3 and 5), given that this interaction is primarily f-based. (Recall in this connection the localized nature of the NMR shielding (eq 4). The $1/r_N^2$ dependence means that MO contributions at the NMR nucleus get the greatest weight in these integrals. In the given case, these contributions are primarily U 5f orbitals, as has been discussed before.)

To summarize, the trends in ^{235}U NMR shielding and chemical shift were studied along the fluoride chloride series (Figure 3). It was found that the observed trend can be explained by changes in the paramagnetic part. This shielding contribution is dominated by the occupied−virtual contribution (eq 3 and Table 6). The occupied−virtual shielding $\sigma^{p,oc-vir}$ is, in turn, dominated by magnetic interactions between uranium 5f-based occupied and virtual orbitals. The strength of the interaction is inversely proportional to the occupied−virtual energy separation (eq 5) and the separation decreases monotonically along the series. This turns out to be the major factor for the observed trend in the shielding. In addition, the amount of f-character in the occupied MOs increases along the series. This leads to better overlap (increase in the magnetic interaction) and is a second factor responsible for the shielding trend. Finally, note that very similar factors should be responsible for the shielding trend in the methoxy compounds $UF_{6-n}(OCH_3)_n$ (Figure 3). Nevertheless, neither the occupied−virtual gap nor the percentage f-character should change as strongly as for the fluoride chlorides, leading to a more modest change of the shielding along the series.

6. Conclusions

In Parts 1 and 2 of this series,[39] relativistic quantum mechanics (DFT) were applied to the calculation of NMR shieldings and chemical shifts in diamagnetic actinide compounds. These studies, together with preliminary reports,[40,41] extend the applicability of first-principle quantum mechanics considerably. Indeed, systems containing any particular nucleus can now be studied for the first time. Thus, the entire periodic table is becoming accessible to the theoretical first principle study of NMR parameters.

In the first paper of the series,[39] various aspects and issues related to the application of NMR methods to actinide complexes were discussed and evaluated. In the given second paper, I have built on these results and applied the methods to a wide range of diamagnetic uranium compounds. In particular, uranyl systems $[UO_2L_n]^{\pm q}$, inorganic UF_6 derivatives ($UF_{6-n}Cl_n$; see also Part 1), and organometallic complexes $[UF_{6-n}(OCH_3)_n]$ have been discussed. For these systems, theoretical shieldings and chemical shifts have been compared to experiment where possible. This is principally only the case for the ligand NMR. In these cases, moderate (e.g., ^{19}F NMR chemical shifts in $UF_{6-n}Cl_n$) to excellent agreement [e.g., ^{19}F chemical shift tensor in UF_6, Part 1, or ^{1}H NMR in $UF_{6-n}(OCH_3)_n$] was found between theory and experiment. Possible reasons for the remaining shortcomings

have been discussed, although no definite explanation could be provided at this point. Nevertheless, the success of the theoretical methods (even if somewhat limited still) gives some confidence in the power of relativistic DFT to predict the NMR in actinide complexes.

With this confidence, I have used these methods to predict ^{235}U NMR shieldings and chemical shifts. As has been discussed before, experimental NMR does not exist for the ^{235}U nucleus or for any other actinide nucleus. For instance, plutonium (^{239}Pu) is about the only spin-1/2 nucleus in the entire periodic table that has not been observed by NMR. Part of the experimental difficulty is the large chemical shift range for these nuclei. The predicted chemical shift range is rather large indeed. A range of 21 000 ppm for the 23 molecules studied (Table 5) was calculated. The chemical shift range is, in fact, likely to be even larger if more molecules such as UBr_6 were included. At that point, theory has the potential of supporting and guiding experimental studies. Thus, the calculated numbers (Table 5) could be used to narrow down the chemical shift range that would have to be scanned for a signal. This, then, should lead to a more focused experimental search and consequently to improved signal-to-noise ratios.

The influence of spin−orbit effects[18,33] on the calculated NMR in uranium compounds was discussed. In Part 1, spin−orbit effects were studied for the ligand NMR. There, it was found that spin−orbit is clearly relevant in some cases but could have been neglected in others. In the given paper, these studies were extended to the NMR of the uranium metal. It was found that spin−orbit had a very large influence on the calculated ^{235}U shieldings and a modest but certainly not negligible influence on the relative chemical shifts. It was argued that the influence of spin−orbit on the chemical shifts could become much more prominent for systems with heavy ligand nuclei or for molecules with more than one actinide center—these are cases that had not been considered in this study. In summary, I conclude that spin−orbit cannot be neglected for the NMR of the actinide nucleus.

The connection between calculated NMR shieldings (chemical shifts) and the electronic structure, i.e., the factors determining trends in the chemical shifts were analyzed in detail. As a representative example, the ^{235}U NMR in $UF_{6-n}L_n$ compounds (L = Cl, but also OCH_3; $n = 0-6$) (Figure 3) was chosen. For these compounds, a large increase in chemical shift has been traced to an increase in magnitude of the (negative) paramagnetic shielding contribution (Table 6). The paramagnetic shielding is, in turn, dominated by magnetic couplings between occupied and virtual MOs. It was found that in the given case, the principal transitions (couplings) involve occupied and virtual MOs that possess U 5f character. Along the fluoride chloride series $UF_{6-n}Cl_n$, the occupied−virtual separation for the f-containing orbitals decreases strongly for increasing n (Figure 4).[74] This is the major factor that sets the trend in the calculated ^{235}U NMR. Additionally, the amount of f-character in the occupied MOs increases along the series, from 18.0% to 21.5%,[74] and this leads to better overlap between the occupied and virtual MOs involved. This is the other, minor factor that has an influence on the ^{235}U NMR chemical shifts. The trend and underlying reason is expected to be similar, although less pronounced, for the methoxy series $UF_{6-n}(OCH_3)_n$.

Limitations and possible future directions of existing DFT-NMR methods have been discussed elsewhere.[5] Besides the issues discussed in this paper,[5] it will be necessary to develop the theory and computational methods for paramagnetic molecules. Such paramagnetic molecules are prevalent in actinide chemistry, in particular in the organometallic chemistry of these elements. Typically, the unpaired electron(s) occupy various, formally nonbonding f-levels. In many cases, ligand NMR signals have been obtained for such species (e.g., refs 100 and 101). Current theory is, however, unable to model the NMR shielding or chemical shift in these open shell systems. Thus, for theory to become truly useful in this area of chemistry (as well as for transition metal complexes), it shall be necessary to extend existing NMR methods toward open shell systems. Principally, this requires that one treat the interaction of the magnetic perturbation with the spin ($\vec{s}\cdot\vec{B}$ terms) and orbital angular momentum ($\vec{l}\cdot\vec{B}$ terms similar to the closed shell case, eqs 3−5) on an equal footing.

Acknowledgment. The author would like to thank P. J. Hay and R. L. Martin for their support and for countless discussions and encouragement. He would like to acknowledge D. W. Keogh, M. P. Neu, and D. L. Clark, for help with some of the experimental data, and W. A. de Jong, for his insight and for providing data prior to publication. The author is grateful to S. K. Wolff and T. Ziegler, coauthors of Part 1, for ongoing discussion and for making their NMR programs available prior to public release. He further acknowledges funding from the Laboratory Directed Research and Development program of the Los Alamos National Laboratory, operated by the University of California under contract to the US Department of Energy (W-7405-ENG-36), and from the Seaborg Institute for Transactinium Science at Los Alamos. Finally, a few calculations have been performed at the CLRC Daresbury Laboratory also.

Supporting Information Available: Tables S1−S8 containing optimized geometries for $[UO_2(H_2O)_5]^{2+}$ and $[UO_2(CO_3)_3]^{4+}$ (Tables S1−S3), calculated ^{13}C and ^{17}O shieldings in methoxy compounds $UF_{6-n}(OCH_3)_n$ (Table S4), some data that is relevant to Figure 4 (Table S5), as well as calculated NMR shieldings for distorted geometries of $[UO_2(H_2O)_5]^{2+}$, $UF_5(OCH_3)$, and UF_6 (Tables S6−S8).This material is available free of charge via the Internet at http://pubs.acs.org.

IC020370J

(100) Luke, W. D.; Streitwieser, A. In *Lanthanide and Actinide Chemistry and Spectroscopy;* ACS Symposium Series 131; Edelstein, N. M., Ed.; American Chemical Society: Washington, DC, 1980; pp 93−140.

(101) Fischer, R. D. In *Fundamental and Technological Aspects of Organo-f-Element Chemistry;* NATO ASI C155; Marks, T. J., Fragalà, I. L., Eds.; D. Reidel: Dordrecht, The Netherlands, 1985; pp 277−326.